Mitogen-Induced Activation of Na^+/H^+ Exchange in Vascular Smooth Muscle Cells Involves Janus Kinase 2 and Ca^{2+}/Calmodulin†

Maria N. Garnovskaya,* Yurii V. Mukhin, Justin H. Turner, Tamara M. Vlasova, Michael E. Ullian, and John R. Raymond

Medical and Research Services, Ralph H. Johnson Veterans Affairs Medical Center, and Department of Medicine (Nephrology Division), Medical University of South Carolina, Charleston, South Carolina 29425

Received April 9, 2003; Revised Manuscript Received April 29, 2003

ABSTRACT: The sodium/proton exchanger type 1 (NHE-1) plays an important role in the proliferation of vascular smooth muscle cells (VSMC). We have examined the regulation of NHE-1 by two potent mitogens, serotonin (5-HT, 5-hydroxytryptamine) and angiotensin II (Ang II), in cultured VSMC derived from rat aorta. 5-HT and Ang II rapidly activated NHE-1 via their G protein-coupled receptors ($5\text{-}HT_{2A}$ and AT_1) as assessed by proton microphysiometry of quiescent cells and by measurements of intracellular pH on a FLIPR (fluorometric imaging plate reader). Activation of NHE-1 was blocked by inhibitors of phospholipase C, CaM, and Jak2 but not by pertussis toxin or inhibitors of protein kinase C. Immunoprecipitation/immunoblot studies showed that 5-HT and Ang II induce phosphorylation of Jak2 and induce the formation of signal transduction complexes that included Jak2, CaM, and NHE-1. The cell-permeable Ca^{2+} chelator BAPTA-AM blocked activation of Jak2, complex formation between Jak2 and CaM, and tyrosine phosphorylation of CaM, demonstrating that elevated intracellular Ca^{2+} is essential for those events. Thus, mitogen-induced activation of NHE-1 in VSMC is dependent upon elevated intracellular Ca^{2+} and is mediated by the Jak2-dependent tyrosine phosphorylation of CaM and subsequent increased binding of CaM to NHE-1, similar to the pathway previously described for the bradykinin B_2 receptor in inner medullary collecting duct cells of the kidney [Mukhin, Y. V., et al. (2001) *J. Biol. Chem. 276*, 17339−17346]. We propose that this pathway represents a fundamental mechanism for the rapid regulation of NHE-1 by $G_{q/11}$ protein-coupled receptors in multiple cell types.

The ubiquitously expressed, amiloride-sensitive sodium/proton exchanger type 1 (NHE-1)[1] is activated by various stimuli, including growth factors, mitogens, integrins, and hyperosmolarity, and plays an essential role in pH regulation, volume homeostasis, cell growth, and differentiation (*1*, *2*). An important role for the Na^+/H^+ exchange in vascular smooth muscle cell (VSMC) growth has been described previously (*3*, *4*). In cultured VSMC, growth factors cause a proliferative response that is associated with activation of Na^+/H^+ exchange (*5*).

NHE-1 is a phosphoglycoprotein of 815 amino acids that contains high- and low-affinity Ca^{2+}/calmodulin-binding sites and several potential phosphorylation sites (*2*, *6*). The structure of NHE-1 suggests that its regulation can occur through at least three mechanisms: (1) interaction of a regulatory factor(s) with a critical cytoplasmic region of NHE-1, (2) direct phosphorylation of serines and possibly threonines or tyrosines located in the cytoplasmic domains, and (3) Ca^{2+}/calmodulin binding (*2*). Several protein kinases have been proposed to regulate NHE-1, including Ca^{2+}/calmodulin-dependent kinase (*7*), protein kinase C (*8*, *9*), p160 Rho-associated kinase (*10*), phosphatidylinositol 3′-kinase (*9*), and members of the mitogen-activated protein kinase (MAPK) family (*2*, *8*, *11*−*13*). In VSMC, the 90 kDa S6 kinase ($p90^{rsk}$) can directly phosphorylate NHE-1 on $serine^{703}$ and mediate an increase in Na^+/H^+ exchange (*14*, *15*). The rapid activation of NHE-1 by mitogens is usually associated with an increase in its phosphorylation (*16*). However, deletion of the region of NHE-1 with most of the potential phosphorylation sites (amino acids 636−815)

† This work was supported by grants from the Department of Veterans Affairs (Merit Awards to M.N.G. and J.R.R. and a REAP Award to J.R.R., Y.V.M., and M.N.G.), the National Institutes of Health (DK52448 to J.R.R. and K01-DK02694 to Y.V.M.), laboratory endowments jointly supported by the MUSC Division of Nephrology and Dialysis Clinics, Incorporated (M.E.U. and J.R.R.), an American Heart Association fellowship award (Y.V.M.), and a MUSC University Research Foundation award (M.N.G.). The FLIPR is a shared MUSC resource obtained with Grant S10RR013005 from the U.S. Public Health Service. The Cytosensor microphysiometer is a shared VA resource obtained with a VA large equipment grant.

* To whom correspondence should be addressed at the Medical University of South Carolina, 96 Jonathan Lucas St., Room 829 CSB, P.O. Box 250623, Charleston, SC 29425-2227. Telephone: (843) 876-5128 or (843) 789-6776. Fax: (843) 876-5129 or (843) 792-8399. E-mail: garnovsk@musc.edu.

[1] Abbreviations: Ang II, angiotensin II; BAPTA-AM, 1,2-bis(2-aminophenoxy)ethane-*N*,*N*,*N*′,*N*′-tetraacetic acid acetoxymethyl ester; BCECF, 2′,7′-bis(2-carboxyethyl)-5- (and 6-) carboxyfluorescein; CaM, calmodulin; ECAR, extracellular acidification rate; EIPA, 5-(*N*-ethyl-*N*-isopropyl)amiloride; ERK, extracellular signal regulated protein kinase; F12, Ham's F12 nutrient mixture; FLIPR, fluorometric imaging plate reader; HBSS, Hank's balanced salt solution; 5-HT, 5-hydroxytryptamine (serotonin); Jak2, Janus kinase 2; LPA, lysophosphatidic acid; MAPK, mitogen-activated protein kinase; MEM, minimal essential medium; NHE, Na^+/H^+ exchanger; PBS, phosphate-buffered saline; PKC, protein kinase C; PLC, phospholipase C; PMA, phorbol 12-myristate 13-acetate; RIPA, radioimmune precipitation buffer; TMA, tetramethylammonium; VSMC, vascular smooth muscle cells.

10.1021/bi034563+ CCC: $25.00
Published on Web 05/20/2003

preserves ~50% of the response to growth factors, indicating that direct phosphorylation of NHE-1 is not sufficient for its full activation (*17*). Recently, we described a novel pathway for the activation of NHE-1 by the bradykinin B_2 receptor in the mIMCD-3 cell (a murine cell culture model of the kidney inner medullary collecting duct), which involves Janus kinase 2 (Jak2) mediated tyrosine phosphorylation of CaM and subsequent increased binding of CaM to NHE-1 (*18*).

NHE-1 may play a key role in the maintenance of blood pressure in that increased activity of NHE-1 has been observed in cells and tissues from hypertensive animals and humans (*19*−*21*). Northern blot analysis showed that cultured VSMC from Sprague-Dawley and Wistar-Kyoto rats express only the NHE-1 isoform and that steady-state mRNA levels are similar for normal and spontaneously hypertensive animals (*21*, *22*). In addition, no mutations in the NHE-1 DNA sequence have been found in hypertensive animals, suggesting that increased activity of the antiporter is caused by an alteration in the regulation of NHE-1 (*21*).

Because vascular smooth muscle cells are critical for maintaining vascular tone and blood pressure, we studied the regulation of NHE-1 activity in rat aortic VSMC by two mitogens, angiotensin II (Ang II) and serotonin (5-HT), in this report. Ang II, a potent hypertrophic factor for VSMC, mediates its effects via specific plasma membrane Ang II receptors that belong to the seven membrane-spanning G protein-coupled receptor family. In rat aortic VSMC, Ang II receptors were found to be of the AT_1 subtype (*23*). Ang II stimulates multiple signaling pathways (reviewed in ref *24*) including MAPKs, Src family kinases, phospholipase D, and Janus kinases (*25*−*30*). Ang II has also been shown to stimulate NHE-1 activity in VSMC (*31*, *32*) but does not appear to increase the steady-state levels of NHE-1 mRNA (*33*). The precise mechanism of NHE-1 activation by Ang II remains unclear, although there is evidence for involvement of both PKC-dependent and PKC-independent pathways (*31*), as well as tyrosine kinase-dependent pathways (*34*). A role for p38 and ERK1/2 in Ang II-mediated regulation of NHE-1 in VSMC has also been suggested (*11*).

Although 5-HT appears to play an important role in cardiovascular disease and hypertension (*35*−*37*), there are few existing studies into its mechanisms of action in VSMC. A high level of expression of 5-HT type 2 receptor mRNA has been demonstrated in cultured rat aortic VSMC (*38*). In addition, despite the presence of mRNA for other 5-HT receptors, the 5-HT_{2A} receptor is the only serotonin receptor in rat aortic VSMC that has been demonstrated to be functionally active (*39*). Previous reports have shown that 5-HT can stimulate protein tyrosine phosphorylation and increase intracellular Ca^{2+} in cultured canine femoral arterial smooth muscle cells (*40*) and that the 5-HT_{2A} receptor can activate ERK in VSMC (*41*). The mitogenic effect of 5-HT in VSMC may be mediated by Src family tyrosine kinases, PKC, and/or the MAPK pathway (*42*). There are no data on the mechanism of regulation of NHE-1 by 5-HT in VSMC, although we and others have shown stimulation of NHE-1 by 5-HT in fibroblasts and mesangial cells (*43*−*46*).

In the current study, we used proton microphysiometry of quiescent VSMC and measurements of intracellular pH on a FLIPR to study acute Ang II- and 5-HT-induced activation of NHE-1 in VSMC. The major purpose of this study was to delineate key components of a signal transduction pathway that leads to the activation of NHE-1 by those mitogens. Our findings support a critical role for Jak2-induced phosphorylation of CaM in the process of the activation of NHE-1 by both Ang II and 5-HT in VSMC and suggest that this pathway may represent a fundamental mechanism for the rapid regulation of NHE-1 by $G_{q/11}$-coupled receptors in multiple cell types.

EXPERIMENTAL PROCEDURES

Materials. Fluo-3 and BCECF [2′,7′-bis(2-carboxymethyl)-5(6)-carboxyfluorescein] were purchased from Molecular Probes (Eugene, OR). Ketanserin and 5-(*N*-ethyl-*N*-isopropyl)amiloride were purchased from RBI (Natick, MA). ET-18-OCH_3, AG-490, and D609 were from Biomol (Plymouth Meeting, PA). Angiotensin II, 5-hydroxytryptamine, lysophosphatidic acid (LPA), tetramethylammonium (TMA) chloride, probenecid, phorbol 12-myristate 13-acetate, and various salts were from Sigma (St Louis, MO). BAPTA-AM [1,2-bis(2-aminophenoxy)ethane-*N*,*N*,*N*′,*N*′-tetraacetic acid acetoxymethyl ester], calmidazolium, fluphenazine, W-7, GF109203X, ophiobolin, PD98059, and anti-phosphotyrosine monoclonal antibody were from Calbiochem (San Diego, CA). Anti-CaM monoclonal antibody, anti-Jak2 agarose conjugated antibody, and anti-phosphotyrosine polyclonal antibody were from Upstate Biotechnology (Lake Placid, NY). Anti-phosphospecific Jak2 antibody was from Biosource International (Camarillo, CA) or QCB (Hopkinton, MA). Anti-NHE-1 polyclonal antibody was from Chemicon International (Temecula, CA). All cell culture media and supplements were from Life Sciences (Grand Island, NY). Polycarbonate cell culture inserts for microphysiometry and black 96-well microtiter plates for the FLIPR were from Corning Costar (Cambridge, MA). Black pipet tips were from Molecular Devices Corp. (Sunnyvale, CA).

Cell Culture. VSMC were derived from surgical aortic explants from Sprague-Dawley rats and maintained in MEM supplemented with 10% fetal bovine serum, 10 mg/mL streptomycin, and 100 units/mL penicillin at 37 °C in a 5% CO_2-enriched, humidified atmosphere. Cells were used at passages 4−7. Experimental procedures were performed under approved protocols from the Institutional Animal Care and Use Committees of the Ralph. H. Johnson VA Medical Center and the Medical University of South Carolina. Treatment of the animal subjects conformed to guidelines of the American Veterinary Medical Association.

Microphysiometry. We have previously used the Cytosensor microphysiometer (Molecular Devices Corp., Sunnyvale, CA) to study Na^+/H^+ exchange in fibroblasts (*43*, *44*), enterocytes (*47*), and kidney epithelial cells (*18*). The microphysiometer uses a light addressable silicon sensor to detect extracellular protons (*48*). Each of eight channels has two inlet ports for buffers, one for the vehicle control and the other for a test substance. The cells are perfused with buffer, and valve switches and stop−start cycles are totally controlled by a programmable computer. Acidification rate data are transformed by a personal computer running Cytosoft version 2.0 and are presented as extracellular acidification rates (ECAR) in micro-Volts per second, which roughly corresponds to milli-pH units per minute (Nernst equation). To facilitate comparison of data between two

channels, values are expressed as percentages of a baseline determined by computerized analysis of the three data points prior to exposure of the cell monolayers to a test substance.

For all experiments, VSMC were plated onto polycarbonate membranes (3 μm pore size, 12 mm size) at a density of 300000 cells per insert the night prior to experimentation. After attachment to the membranes, cells were growth-arrested in serum-free culture medium for 20 h. On the day of the study, cells were washed with serum-free, bicarbonate-free Ham's F-12 medium, placed into the microphysiometer chambers, and perfused at 37 °C with the same medium or balanced salt solutions. For most studies, the pump cycle was set to perfuse cells for 60 s, followed by a 30 s "pump-off" phase, during which proton efflux was measured from the 8th through the 28th second. Cells were exposed to the test agent for three or four cycles (270−360 s). Valve switches (to add or remove test agents) were performed at the middle of the pump cycle, and data points were acquired every 90 s. The peak effect during stimulation was expressed as the percentage increase over baseline.

Measurement of Intracellular Ca^{2+}. We used a FLIPR (Molecular Devices) fluorometric imaging plate reader system (*49*) to measure intracellular Ca^{2+} in VSMC plated into 96-well microtiter plates. Cells were seeded (∼50000 cells/well) in 96-well clear bottom black microplates (Corning Costar Corp., Cambridge, MA) and left overnight in a CO_2 incubator at 37 °C. On the day of the assay, cells were loaded with 4 μM Fluo-3 for 1 h in Hank's balanced salt solution (HBSS), pH 7.4, containing 20 mM HEPES and 2.5 mM probenecid. After being loaded, cells were washed four times with HBSS on an automated plate washer (Labsystems, Helsinki, Finland) and placed into the FLIPR. All 96 wells were simultaneously illuminated for 0.4 s by an argon laser (488 nm) set at ≈300 mW (Coherent Inc., Santa Clara, CA). Fluorescence emission readings were measured using a 540 nm band-pass filter at 1 s intervals until a baseline was obtained (about 10 readings). Cells were then simultaneously exposed to a range of 5-HT or Ang II concentrations (10^{-5} to 3×10^{-10} M), and fluorescence readings were obtained from each well every second for a total of 2 min and then every 6 s for 3 min. Replicate readings were averaged, and each tracing was normalized against background fluorescence from wells treated with buffer controls. Tracings were acquired, averaged, and normalized using the FLIPR Control software program (Molecular Devices).

Measurement of Intracellular pH. The FLIPR was also used to measure pH_i in VSMC in 96-well microtiter plates. Cells were treated as described above and then loaded with 5 μM BCECF in loading buffer (HBSS, pH 7.4, containing 15 mM HEPES and 1 mM probenecid) for 1 h at 37 °C. Twenty minutes prior to the end of the loading phase, 15 mM NH_4Cl was added to each well. Cells were then washed two times with loading buffer containing 15 mM NH_4Cl and subsequently acid-loaded by an ammonium chloride prepulse protocol, in which the extracellular buffer contains NH_4^+ and NH_3 in an equilibrium that is essentially recapitulated in the cell interior. When the extracellular medium is changed to a buffer lacking NH_4Cl, intracellular NH_3 diffuses rapidly out of the cell, causing the cells to become acutely "loaded" with protons donated from NH_4^+ (*50*). Some cells were pretreated with 50 μM AG-490 or 5 μM EIPA for 20 min. Cells were allowed to recover from the acid load in the presence or absence of sodium and various test substances. Fluorescence excitation was obtained using an argon laser (488 nm wavelength at 300 mW), and emission (∼540 nm) was monitored kinetically. The tracings from at least six wells under the same conditions were averaged, and tracings from the negative controls (wells pretreated with EIPA) were subtracted. The slopes of fluorescence changes were calculated as rate of fluorescence change (fluorescence counts per second).

Immunoprecipitation. Quiescent VSMC monolayers were treated with 100 nM Ang II, 1 μM 5-HT, or vehicle for 10 min and then lysed in 1 mL per 100 mm dish of RIPA buffer (150 mM NaCl, 50 mM Tris-HCl, pH 7.4, 1 mM EDTA, 1% NP-40, 1 mM NaF, 1 mM Na_3VO_4, 1 mM phenylmethanesulfonyl fluoride, and aprotinin, leupeptin, and pepstatin at 1 μg/mL each). Cell lysates were then precleared by incubation with a protein A−agarose bead slurry for 30 min at 4 °C. Precleared lysates (1 μg/μL total cell protein) were incubated with anti-Jak2/protein A−agarose, anti-NHE-1 antibody, or polyclonal anti-phosphotyrosine antibody overnight at 4 °C. Phosphotyrosine and NHE-1 immunoprecipitates were captured by addition of protein A−agarose. The agarose beads were collected by centrifugation, washed three times with RIPA buffer, resuspended in 2× Laemmli sample buffer, and boiled for 5 min. Samples were then subjected to SDS−PAGE followed by subsequent immunoblot analysis with monoclonal anti-CaM or anti-phosphotyrosine IgG. The same Western blots were reprobed with the antibody used for immunoprecipitation to ensure that equal amounts of protein were loaded in each lane.

Jak2 Phosphorylation Assay. Phosphorylation of Jak2 in response to Ang II and 5-HT was assessed using a Jak2 dual phosphospecific antibody. Quiescent cells were treated with 100 nM Ang II, 1 μM 5-HT, or vehicle for 10 min and lysed in RIPA buffer. The lysates were then subjected to SDS−PAGE under reducing conditions using 4−20% precast gels (Novex, San Diego, CA). After semidry transfer to polyvinylidine difluoride membranes, membranes were blocked with Blotto buffer and incubated with phospho-Jak2 antibody (0.5 μg/mL). Following incubation with an alkaline phosphatase-linked secondary antibody, immunoreactive bands were visualized by a chemiluminescent method (CDP Star, New England Biolabs, Beverly, MA) using preflashed Kodak X-AR film and quantified using a GS-670 densitometer and Molecular Analyst software (Bio-Rad, Hercules, CA). To ensure that equal amounts of protein were loaded in each lane, we stripped and reprobed the blots with control Jak2 antibody, which equally recognizes both phosphorylated and nonphosphorylated Jak2.

Statistical Analysis. Data were analyzed for repeated measures by Student's *t* test for unpaired two-tailed analysis. *P* values less than 0.05 were considered significant.

RESULTS

Ang II and 5-HT Stimulate Sodium-Dependent, EIPA-Inhibitable Proton Efflux in VSMC. We used a Cytosensor microphysiometer to measure proton efflux from intact monolayers of VSMC plated onto polycarbonate membranes. Figure 1A shows that 100 nM Ang II (diamonds) or 1 μM 5-HT (circles) rapidly increased the extracellular acidification

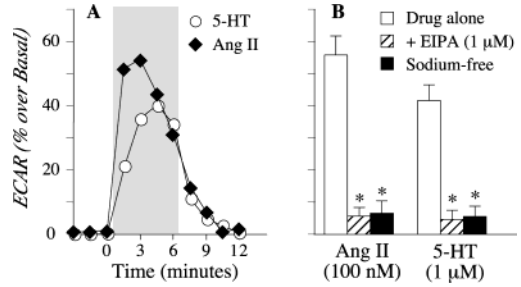

FIGURE 1: 5-HT and Ang II stimulate NHE-1 activity in VSMC. Microphysiometry was performed on quiescent VSMC monolayers as described in Experimental Procedures. Panel A: 1 μM 5-HT (circles) or 100 nM Ang II (diamonds) stimulates the extracellular acidification rate (ECAR). The shaded area represents time during which cells were exposed to hormones. Panel B: ECAR stimulated by 5-HT and Ang II in various buffers including a balanced salt solution containing NaCl with or without 1 μM EIPA and a balanced salt solution with sodium chloride substituted by TMA. All experiments were performed at least five times. Error bars in panel B represent the SEM (*, $P < 0.01$ versus samples treated with agonist alone).

rate (ECAR). Figure 1B shows that the stimulatory effect of Ang II and 5-HT occurred in a sodium-containing balanced salt solution (white bars) but not in a solution in which sodium was replaced by tetramethylammonium (TMA) (black bars). The increases in ECAR also were blocked by the amiloride analogue EIPA, an inhibitor of NHE-1 (hatched bars). Thus, Figure 1 presents evidence that Ang II and 5-HT activate proton efflux in VSMC through stimulation of NHE-1.

Role for a Receptor−G Protein−PLC Pathway in 5-HT- and Ang II-Induced Activation of NHE. In Figure 2A, we examined the effects of various chemical inhibitors on 5-HT- and Ang II-stimulated ECAR in VSMC. Pretreatment of cells for 10 min with ketanserin (a 5-HT_{2A} receptor antagonist) and losartan (an AT_1 receptor antagonist) completely blocked the activation of NHE-1 by 5-HT and Ang II, respectively, suggesting that these mitogens activate NHE-1 through their G protein-coupled receptors. Pretreatment of the cells with 200 ng/mL pertussis toxin (PTX) for 20 h did not impair Ang II- or 5-HT-induced activation of NHE-1, suggesting that PTX-sensitive G protein α subunits are not required for Ang II- and 5-HT-induced NHE-1 activation. The same treatment with PTX nearly completely blocked activation of NHE-1 by 1 μM lysophosphatidic acid (LPA), which has previously been shown to utilize PTX-sensitive intracellular signaling pathways in VSMC (*51*, *52*), indicating that PTX-sensitive $G_{i/o}$ α subunits were indeed inhibited under our experimental conditions.

Two phospholipase C (PLC) inhibitors (D609 and ET-18-OCH_3) attenuated by ≥50% the ability of 5-HT and Ang II to activate proton efflux, suggesting that the 5-HT_{2A} and AT_1 receptors couple to PLC in VSMC.

Lack of Involvement of PKC in 5-HT- and Ang II-Induced Activation of NHE. Because PLC activation can lead to stimulation of protein kinase C (PKC) through the intermediate actions of diacylglycerol, we tested the effects of the PKC inhibitor GF109203X (1 μM) as well as PKC depletion by prolonged exposure of cells to 160 nM phorbol 12-myristate 13-acetate (PMA) on 5-HT- and Ang II-induced ECAR. Those treatments did not attenuate 5-HT- or Ang II-induced ECAR but were able to inhibit PMA- (1 μM) elicited proton

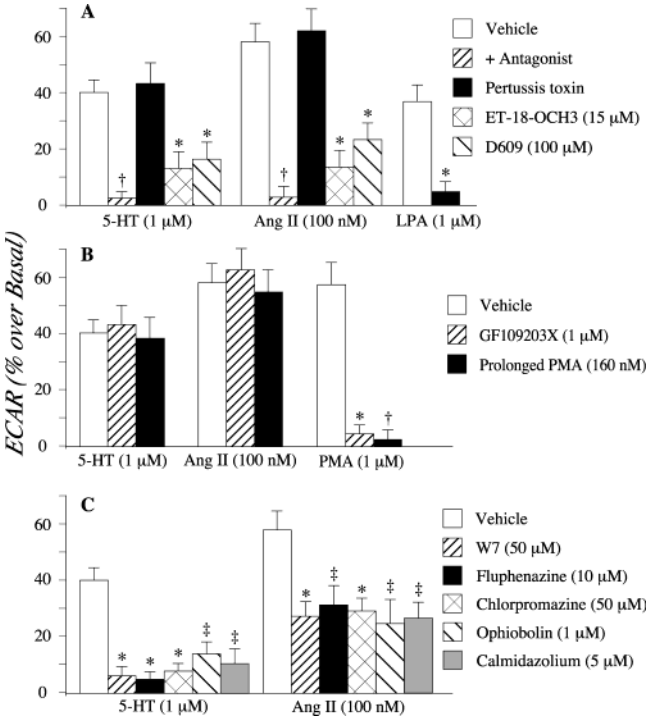

FIGURE 2: Effects of various inhibitors on the activation of ECAR by 5-HT and Ang II. ECAR was measured by microphysiometry as described in Experimental Procedures. Panel A: Cells were preincubated with pertussis toxin (200 ng/mL) overnight prior to stimulation with 1 μM 5-HT or with 100 nM Ang II and with other inhibitors for 30 min prior to stimulation with 1 μM 5-HT or with 100 nM Ang II. Ketanserin is a 5-HT_{2A} receptor antagonist, losartan is an AT_1 receptor antagonist, and D609 and ET-18-OCH_3 are inhibitors of PLC. Panel B: Cells were pretreated with 160 nM PMA for 20 h or with 1 μM GF109203X (PKC inhibitor) for 30 min before stimulation with 1 μM 5-HT, 100 nM Ang II, or 1 μM PMA. Panel C: Cells were preincubated with CaM inhibitors for 30 min prior to addition of 5-HT or Ang II. All experiments were performed at least three times in duplicate or triplicate. Error bars represent the SEM (‡, $P < 0.05$; *, $P < 0.01$; †, $P < 0.005$; versus samples treated with agonist alone).

efflux, showing that those maneuvers blocked PKC in our conditions (Figure 2B). Thus, PKC depletion and a PKC inhibitor, in a concentration that is adequate to block ECAR induced by direct activation of PKC by PMA, do not block 5-HT_{2A} and AT_1 receptor-elicited ECAR (Figure 2B), suggesting that 5-HT_{2A} and AT_1 receptor-elicited ECAR in VSMC is not PKC-dependent.

Inhibitor Studies Suggest the Involvement of CaM in 5-HT- and Ang II-Induced Increases in ECAR. It has previously been shown that both 5-HT_{2A} and AT_1 receptors in VSMC couple to the mobilization of intracellular Ca^{2+} (*53*, *54*). We used a FLIPR plate reader to measure intracellular Ca^{2+} in VSMC and demonstrated that under our experimental conditions 5-HT and Ang II also induced rapid elevations of intracellular Ca^{2+} in VSMC preloaded with 4 μM Fluo-3, a Ca^{2+}-sensitive fluorescent dye (data not shown). Among the targets of increased intracellular Ca^{2+} is Ca^{2+}-dependent calmodulin (CaM), which plays a role in regulating the activity of sodium/proton exchangers through two CaM binding sites located on the carboxyl terminus of NHE-1 (*2*). We hypothesized that CaM may be involved in 5-HT- and Ang II-induced activation of NHE-1 in VSMC. We tested the effects of five structurally distinct CaM inhibitors on 5-HT- and Ang II-activated proton efflux. These experiments

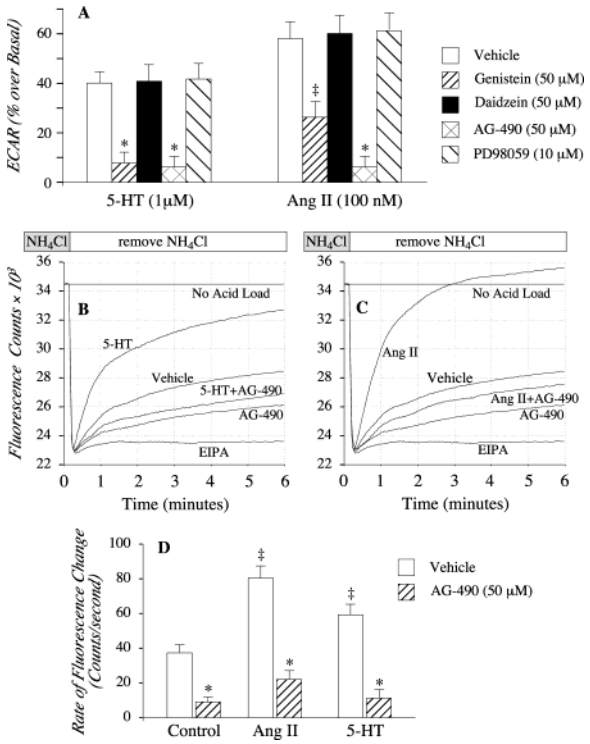

FIGURE 3: Involvement of Jak2 in 5-HT- and Ang II-induced signaling in VSMC. Panel A: ECAR was measured by microphysiometry as described in Experimental Procedures. Tyrosine kinase inhibitors were added 30 min prior to stimulation with 1 μM 5-HT or 100 nM Ang II. Experiments in this panel were performed at least three times in duplicate or triplicate. Error bars represent SEM (‡, $P < 0.05$; *, $P < 0.01$; versus vehicle-treated samples). Panels B and C: Intracellular pH was monitored using BCECF fluorescence as described in Experimental Procedures. Cells were acid-loaded by the ammonium chloride prepulse method and were then allowed to recover in the presence or absence of 1 μM 5-HT (panel B) or 100 nM Ang II (panel C) with or without 1 μM EIPA or 50 μM AG-490 (specific inhibitor of Jak2). The plots are representative of at least six tracings for each condition, all of which showed qualitatively similar results. Panel D: The data were calculated as the average fluorescence tracing from at least six wells after subtraction of signals from negative control wells. The rate of fluorescence change represents the slopes of the fluorescence changes during the first 60 s of recovery. Error bars represent the SEM (‡, $P < 0.05$ versus control; *, $P < 0.01$ versus samples treated with vehicle).

(Figure 2C) showed that W-7 (50 μM), chlorpromazine (50 μM), and fluphenazine (10 μM) each blocked the stimulation of proton efflux elicited by 1 μM 5-HT by ~80%; ophiobolin (1 μM) blocked 5-HT-induced ECAR by ~65% and calmidazolium (5 μM) by ~70%. CaM inhibitors also inhibited Ang II-induced activation of proton efflux, but to a lesser extent, ~50%, suggesting that Ang II may employ some additional, CaM-independent pathways to activate NHE-1. Overall, these studies support a role for CaM in the stimulatory effect of 5-HT and Ang II on NHE-1 in VSMC.

Effects of Inhibitors of Tyrosine Kinase, Janus Kinase 2, and MEK-1 on 5-HT- and Ang II-Induced Increases in ECAR. Because 5-HT and Ang II can also signal through tyrosine kinase pathways and because we have previously established an important role for Jak2 in the regulation of NHE-1 by the bradykinin B_2 receptor in mIMCD-3 cells (*18*), we tested a role of Jak2 in activating NHE-1 in VSMC. In studies with tyrosine kinase inhibitors (Figure 3A), the broad-spectrum tyrosine kinase inhibitor genistein (50 μM) markedly (50−70%) attenuated the ability of 100 nM Ang II or 1 μM 5-HT to stimulate ECAR, whereas the inactive genistein analogue daidzein was without effect. AG-490 (50 μM), a selective inhibitor of the nonreceptor tyrosine kinase Jak2 (*55*), blocked 5-HT- and Ang II-induced ECAR by 80%. The MEK inhibitor PD98059, in concentrations up to 100 μM, was unable to block 5-HT- and Ang II-induced proton efflux. In contrast, preincubation of VSMC with 10 μM PD98059 for 30 min completely blocked 5-HT- and Ang II-induced activation of ERK1/2, documenting inhibition of MEK under our experimental conditions (data not shown). These results suggest involvement of the nonreceptor tyrosine kinase Jak2 in the regulation of NHE-1 in VSMC (Figure 3A).

5-HT and Ang II Stimulate a Sodium-Dependent, EIPA-Inhibitable pH_i Recovery Pathway in VSMC via Jak2. We confirmed the microphysiometer measurements using a second method of studying NHE-1 activity by monitoring intracellular pH (pH_i) using a FLIPR system. VSMC were acid-loaded using the ammonium chloride prepulse method and were then allowed to recover in the presence of 5-HT or Ang II, with or without additions of 5 μM EIPA or 50 μM AG-490. In Figure 3, 1 μM 5-HT (B, left panel) and 100 nM Ang II (C, right panel) accelerated the rate of recovery from an acid load, and these effects were nearly completely inhibited by addition of 5 μM EIPA. Pretreatment with 50 μM AG-490 reduced the rate of recovery from an acid load as well as the maximum amount of recovery during the assay period. In Figure 3D we presented the slopes of the rate of recovery from an acid load during the first 60 s of recovery calculated as rate of fluorescence change. Thus, results presented in Figure 3B−D support the presence of a mitogen-activated, EIPA-inhibitable, pH_i recovery pathway in VSMC and support a role for Jak2 in 5-HT- and Ang II-mediated activation of NHE-1.

5-HT and Ang II Induce Tyrosine Phosphorylation of Jak2, Formation of a Complex between Jak2 and CaM, and Tyrosine Phosphorylation of CaM. To confirm the involvement of Jak2 in 5-HT- and Ang II-mediated signaling, we measured the activation of Jak2 by 5-HT and Ang II using Western blotting with a phosphospecific anti-Jak2 antibody. Treatment with 5-HT (1 μM for 10 min) and with Ang II (100 nM for 10 min) induced an ~150% increase in the level of phosphorylation of Jak2 (Figure 4A).

We next examined whether 5-HT and Ang II could induce a physical interaction between Jak2 and CaM. We explored this possibility using immunoprecipitation of lysates from cells treated with vehicle, 5-HT, or Ang II with anti-Jak2/protein A−agarose, followed by Western blotting with a CaM antibody. Figure 4B shows that CaM and Jak2 co-immunoprecipitate and that their association can be increased by treatment of VSMC with 5-HT or Ang II. Pretreatment of cells with a Jak2 inhibitor, AG-490 (50 μM for 30 min), significantly decreased the amount of CaM in Jak2 immunoprecipitates (Figure 4B), suggesting that 5-HT- and Ang II-induced Jak2 activity is necessary for formation of the complex.

We next considered that 5-HT and Ang II could stimulate tyrosine phosphorylation of CaM. Cells were treated with 1 μM 5-HT, 100 nM Ang II, or vehicle for 10 min, and cell lysates were immunoprecipitated with a polyclonal phosphotyrosine antibody as described in Experimental Proce-

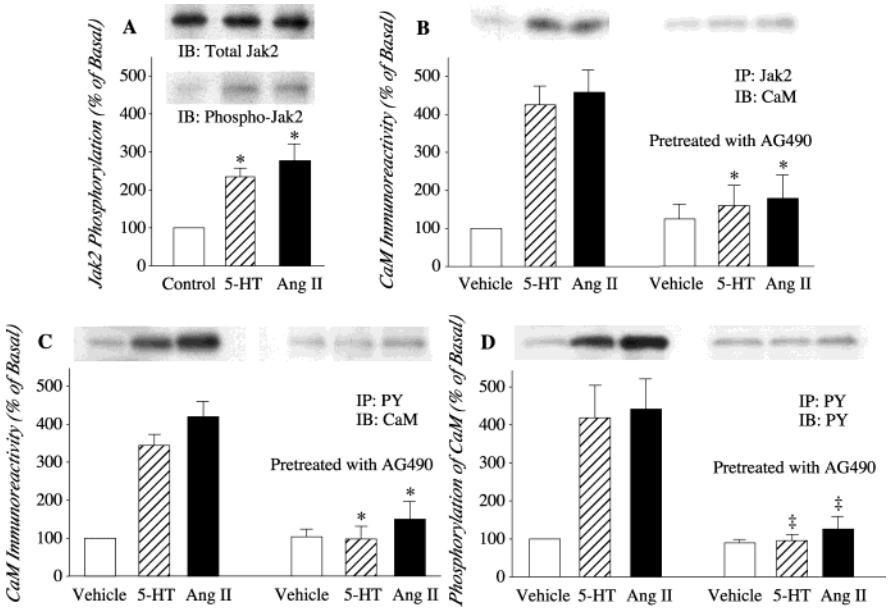

FIGURE 4: Effects of 5-HT and Ang II on Jak2, CaM, and NHE-1. Panel A: 5-HT and Ang II induce tyrosine phosphorylation of Jak2. Cells were treated with 1 μM 5-HT, 100 nM Ang II, or vehicle, lysed, and subjected to immunoblot. The inset is a representative immunoblot (phospho-Jak2). The same blot was stripped and reprobed with antibodies for total Jak2 to ensure equal loading of protein samples (total Jak2). Panel B: Physical association between Jak2 and CaM in the 5-HT- and Ang II-induced signaling complex. Co-immunoprecipitations were performed as described in Experimental Procedures. Experiments show that 1 μM 5-HT or 100 nM Ang II induces a complex that includes CaM and Jak2. Formation of this complex was prevented by preincubation with AG-490 (50 μM) for 30 min. Panel C: This panel shows that 5-HT and Ang II increased the CaM present in phosphotyrosine (PY) immunoprecipitates. The inset shows a representative immunoblot from PY immunoprecipitates. Immunoprecipitation was performed with polyclonal PY antibody, whereas a CaM antibody was used for immunoblotting. The increase in the amount of CaM in PY immunoprecipitates was prevented by preincubation with AG-490 (50 μM) for 30 min. Panel D: Tyrosine phosphorylation of CaM. Immunoprecipitation was performed with polyclonal PY antibody, whereas monoclonal PY antibody was used for immunoblotting. The inset shows a band of the same relative mobility as CaM on a PY immunoblot from PY immunoprecipitates. The blot was stripped and reprobed with a CaM antibody to confirm that the protein that is tyrosine-phosphorylated in response to 5-HT and Ang II is indeed CaM (not shown). Tyrosine phosphorylation of CaM was prevented by preincubation with AG-490 (50 μM) for 30 min. Error bars represent the SEM (‡, $P < 0.05$; *, $P < 0.01$; versus vehicle-treated samples).

dures. Subsequent immunoblot analyses were performed with monoclonal anti-CaM antibodies. The data presented in Figure 4C demonstrate that 5-HT and Ang II increase the amount of CaM in phosphotyrosine immunoprecipitates and that this effect can be significantly decreased by pretreatment of cells with AG-490 (50 μM for 30 min). However, because these data could also reflect the ability of CaM to complex with a tyrosine-phosphorylated protein upon agonist stimulation, we performed another set of experiments aimed to demonstrate the tyrosine phosphorylation of CaM in response to 5-HT and Ang II treatment. Cells were treated with agonists, lysed, and immunoprecipitated with a polyclonal phosphotyrosine antibody as described in Experimental Procedures. Subsequent immunoblot analysis was performed with monoclonal anti-phosphotyrosine immunoglobulin and revealed a band of the same relative mobility as CaM on a phosphotyrosine immunoblot. The same blot was stripped and reprobed with a CaM antibody to confirm the identity of the tyrosine-phosphorylated band as CaM. Thus, the data presented in Figure 4D confirm that CaM becomes tyrosine-phosphorylated in response to 5-HT and Ang II and that tyrosine phosphorylation can be significantly decreased by pretreatment of cells with AG-490 (50 μM for 30 min), suggesting that phosphorylation is induced by Jak2.

CaM Is Present in NHE-1 Immunoprecipitates. To establish whether NHE-1 is present in the mitogen-induced signaling complex, we performed co-immunoprecipitation experiments in which NHE-1 was immunoprecipitated from lysates of untreated VSMC and cells treated with 5-HT or Ang II. Immunoprecipitates were then probed with CaM antibodies. Figure 5A shows that CaM is present in NHE-1 immunoprecipitates and that increasing amounts of CaM complex with NHE-1 after treatment of VSMC with 100 nM Ang II or with 1 μM 5-HT.

NHE-1 Is Present in Jak2 Immunoprecipitates. We performed co-immunoprecipitation experiments in which Jak2 was immunoprecipitated from lysates of VSMC treated or not with 5-HT or Ang II. Immunoprecipitates were next probed with monoclonal NHE-1 antibodies. The immunoblot in Figure 5B documents the presence of NHE-1 in Jak2 immunoprecipitates and shows that the amount of NHE-1 complexed with Jak2 increases after stimulation of VSMC with 5-HT or Ang II. The same blot was stripped and reprobed with CaM antibody, demonstrating an increase in the amount of CaM complexed with Jak2 after stimulation with 5-HT and Ang II (not shown). Thus, 5-HT and Ang II stimulate formation of a complex which includes Jak2, NHE-1, and CaM.

Elevation of Intracellular Ca^{2+} Is Essential for the Complex Formation between Jak2 and CaM and for Tyrosine Phosphorylation of CaM. We have previously suggested that elevated intracellular Ca^{2+} in mIMCD-3 cells contributes to the activation of Jak2, which subsequently phosphorylates CaM, thus modulating the binding of CaM to NHE-1 (*18*). Therefore, in the current study we considered a potential role for Ca^{2+} in the 5-HT- and Ang II-induced activation of NHE-1 in VSMC. Pretreatment of VSMC with BAPTA-AM, a cell-permeable Ca^{2+} sequestrant, nearly completely pre-

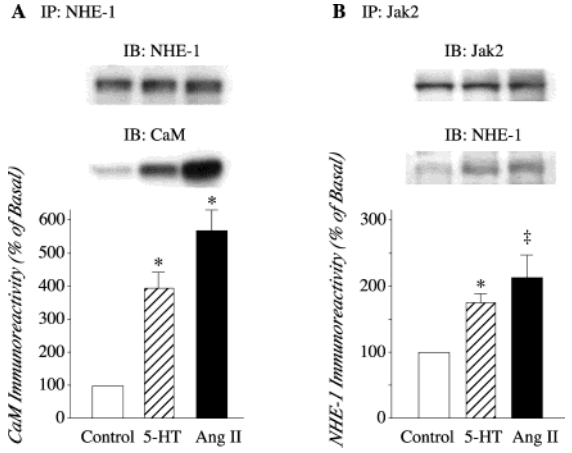

FIGURE 5: 5-HT- and Ang II-induced complex formation between NHE-1, CaM, and Jak2 in VSMC. Panel A: 5-HT and Ang II induce the formation of a complex between CaM and NHE-1. Co-immunoprecipitations were performed as described in Experimental Procedures. Treatment with 1 μM 5-HT or 100 nM Ang II for 10 min increased the amount of CaM in NHE-1 immunoprecipitates. The inset is a representative immunoblot. The same blot was stripped and reprobed with monoclonal antibodies for NHE-1 to ensure an equal loading of protein samples on a gel. Panel B: 5-HT and Ang II induce the formation of a complex between Jak2 and NHE-1. Immunoprecipitations with anti-Jak2/protein A−agarose were performed as described in Experimental Procedures. Treatment with 1 μM 5-HT or 100 nM Ang II for 10 min increased the amount of NHE-1 in Jak2 immunoprecipitates. The inset is a representative immunoblot. The same blot was stripped and reprobed with antibodies for Jak2 to ensure an equal loading of protein samples on a gel. All experiments were repeated at least three times. Error bars represent the SEM (‡, $P < 0.05$; *, $P < 0.01$; versus vehicle-treated samples).

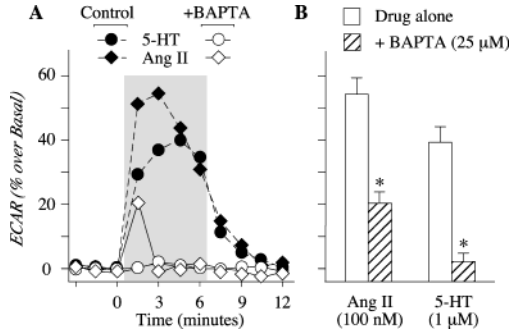

FIGURE 6: Role of Ca^{2+} in 5-HT- and Ang II-induced activation of ECAR in VSMC. Experiments show the effects of BAPTA-AM on the activation of ECAR by 1 μM 5-HT and 100 nM Ang II. ECAR was measured by microphysiometry as described in Experimental Procedures. Cells were preincubated with 25 μM BAPTA-AM for 30 min prior to addition of 5-HT and Ang II. Panel A shows representative tracings from each of the four conditions from different microphysiometer chambers. All experiments were performed at least three times in duplicate, and data presented in panel B are pooled from all experiments performed for each condition. Error bars represent SEM (*, $P < 0.01$ versus samples treated with drug alone).

vented the increase in ECAR induced by 5-HT and significantly (>60%) decreased the Ang II-stimulated increase in ECAR as measured by microphysiometry, suggesting an important role for Ca^{2+} in this pathway (Figure 6).

We next studied a potential role for Ca^{2+} in the 5-HT- and Ang II-induced interaction between Jak2 and CaM. Elevation of intracellular Ca^{2+} by incubation of VSMC with the calcium ionophore A23187 (1 μM) caused an ~150%

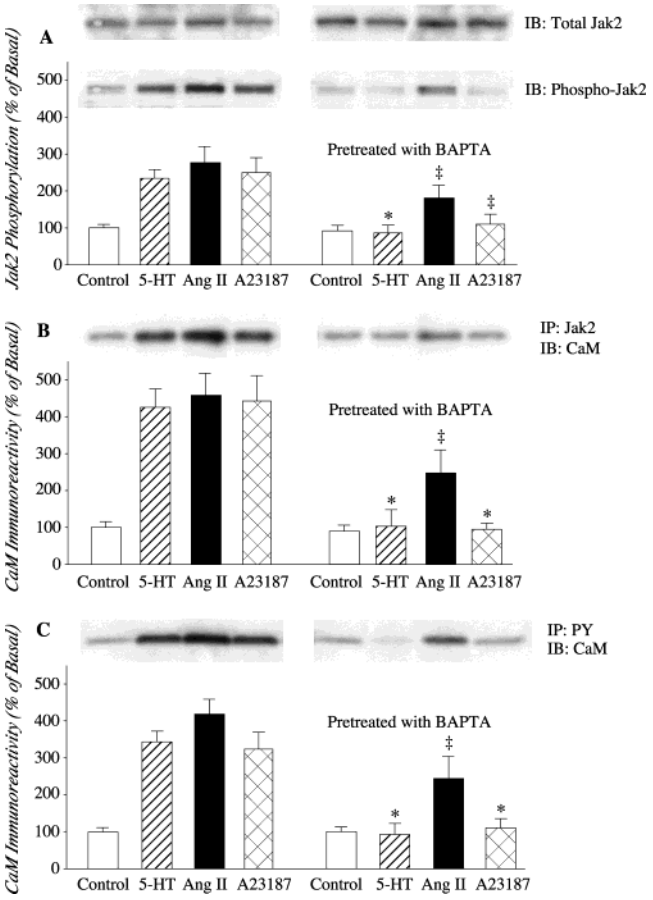

FIGURE 7: Role of Ca^{2+} in 5-HT- and Ang II-induced signaling in VSMC. Panel A: Increased intracellular Ca^{2+} induces tyrosine phosphorylation of Jak2. The phosphorylation state of Jak2 was determined in whole cell lysates from VSMC using a phosphorylation state-specific antibody for Jak2 as described in Experimental Procedures. Cells were treated with 1 μM calcium ionophore A23187, 1 μM 5-HT, 100 nM Ang II, or vehicle, lysed, and subjected to immunoblot. The inset is a representative immunoblot (phospho-Jak2). The same blot was stripped and reprobed with antibodies for total Jak2 to ensure an equal loading of protein samples on a gel (total Jak2). The phosphorylation of Jak2 induced by 5-HT, Ang II, and A23187 was attenuated by pretreatment with BAPTA-AM (25 μM for 30 min). Panel B: Co-immunoprecipitation experiments show that 5-HT, Ang II, and A23187 induce formation of a complex that includes CaM and Jak2. Formation of this complex was attenuated by preincubation with BAPTA-AM (25 μM) for 30 min. Panel C shows that 5-HT, Ang II, or A23187 increases the amount CaM present in phosphotyrosine (PY) immunoprecipitates and that pretreatment with BAPTA-AM (25 μM for 30 min) attenuates tyrosine phosphorylation of CaM. Co-immunoprecipitations were performed as described in Experimental Procedures. Experiments in all panels were repeated three times. Error bars represent the SEM (‡, $P < 0.05$; *, $P < 0.01$; versus vehicle-treated samples).

increase in Jak2 phosphorylation in VSMC that was nearly completely inhibited by pretreatment of the cells with BAPTA-AM (25 μM for 30 min) (Figure 7A). Interestingly, BAPTA-AM also completely prevented phosphorylation of Jak2 induced by 5-HT and partially but significantly (~50%) inhibited Ang II-induced Jak2 phosphorylation (Figure 7A). Exposure of VSMC to A23187, 5-HT, or Ang II for 10 min also increased the amount of CaM in Jak2 immunoprecipitates by ~350% (Figure 7B). Pretreatment of VSMC with 25 μM BAPTA-AM for 30 min completely abolished the increase of CaM in Jak2 immunoprecipitates induced by 1

μM A23187 and 5-HT and partially but significantly (>60%) decreased the amount of CaM in Jak2 immunoprecipitates induced by Ang II (Figure 7B). Thus, in VSMC, Ca^{2+} increases Jak2 phosphorylation and induces formation of a complex between CaM and Jak2.

The next series of experiments were designed to probe the role of Ca^{2+} in the tyrosine phosphorylation of CaM. Cells were pretreated with vehicle or with 25 μM BAPTA-AM for 30 min, then treated with 1 μM 5-HT, 100 nM Ang II, 1 μM A23187, or vehicle for 10 min, and lysed. The cell lysates were immunoprecipitated with a polyclonal anti-phosphotyrosine antibody as described in Experimental Procedures. Subsequent immunoblot analyses were performed with monoclonal anti-CaM antibodies. 5-HT, Ang II, and A23187 each increased tyrosine phosphorylation of CaM by at least 250%. Pretreatment with BAPTA-AM nearly completely blocked A23187- and 5-HT-induced tyrosine phosphorylation of CaM and partially but significantly (>60%) decreased Ang II-induced tyrosine phosphorylation of CaM, suggesting that this phosphorylation is Ca^{2+}-dependent (Figure 7C).

DISCUSSION

The current work expands upon our previous study in which we showed that B_2 receptors endogenous to mIMCD-3 cells activate NHE-1 activity through a pathway that involves PLC, elevated intracellular Ca^{2+}, CaM, and Jak2 (*18*). What is new about this work is that we have shown that two potent mitogens, 5-HT and Ang II, also employ a similar pathway to activate NHE-1 in VSMC cultured from rat aorta, indicating that this pathway is not limited to polarized epithelial cells. We demonstrated that stimulation of VSMC with 100 nM Ang II or 1 μM 5-HT leads to a rapid activation of NHE-1, as shown by two independent methods: (1) measurement of ECAR with a Cytosensor microphysiometer (Figure 1) and (2) measurement of intracellular pH on a FLIPR (Figure 3B−D). This signaling pathway utilizes AT_1 and $5\text{-}HT_{2A}$ receptors, in that losartan and ketanserin, selective antagonists for those receptors, prevented activation of NHE-1 by Ang II and 5-HT. The response was not sensitive to pertussis toxin, indicating a lack of involvement of pertussis toxin-sensitive $G_{i/o}$ proteins (Figure 2A). We also found that two different PLC inhibitors (D609 and ET-18-OCH_3) suppressed activation of NHE-1, suggesting that AT_1 and $5\text{-}HT_{2A}$ receptors couple through PLC to NHE-1 in VSMC (Figure 2A). Because PLC activation can lead to stimulation of PKC through the intermediate actions of diacylglycerol, we tested the effects of a PKC inhibitor (GF109203X) as well as of PKC depletion by prolonged exposure of cells to 160 nM PMA on 5-HT- and Ang II-induced ECAR. Those treatments did not block AT_1 or $5\text{-}HT_{2A}$ receptor-elicited ECAR but were able to inhibit PMA-induced increases in ECAR, suggesting that PKC is not involved in 5-HT- and Ang II-induced NHE-1 activation (Figure 2B). PLC activation also leads to an increase in intracellular Ca^{2+}, which in turn can stimulate CaM. Five structurally distinct CaM inhibitors blocked the stimulation of ECAR elicited by 1 μM 5-HT by ~80% while stimulation by 100 nM Ang II was blocked by ~50%, supporting an important role for CaM in the regulation of NHE-1 in VSMC (Figure 2C).

We also used several tyrosine kinase inhibitors to study the possible role of tyrosine kinases in the 5-HT- and Ang II-induced activation of NHE. The broad-spectrum tyrosine kinase inhibitor genistein, but not its inactive analogue (daidzein), blocked mitogen-stimulated ECAR. The selective Jak2 inhibitor (AG-490) effectively blocked 5-HT- and Ang II-stimulated ECAR and the rate of recovery from an acid load, supporting a role for Jak2 in the regulation of NHE-1 in VSMC (Figure 3). Immunoprecipitation/immunoblot studies also revealed that (1) 5-HT and Ang II stimulate the formation of a complex between CaM and Jak2, (2) CaM becomes tyrosine-phosphorylated following stimulation of VSMC with 1 μM 5-HT or 100 nM Ang II for 10 min, (3) CaM phosphorylation depends on Jak2 activity, and (4) stimulation of VSMC with 5-HT or Ang II increases the amount of NHE-1 in Jak2 immunoprecipitates and the amount of CaM in NHE-1 immunoprecipitates (Figures 4 and 5). Thus, our current work suggests that, in VSMC, Jak2 regulates NHE-1 by phosphorylating CaM and subsequently modulating the interaction of CaM with NHE-1.

There is no consensus on a role for Ca^{2+} in regulating Jak2 activity. Our previous studies in mIMCD-3 cells support a role for elevated intracellular Ca^{2+} in both activation of Jak2 and the subsequent phosphorylation of CaM by Jak2, which in turn results in increased binding of CaM to NHE-1 (*18*). This is in direct contrast to a report by Fukami et al., in which they reported in vitro experiments that showed that Ca^{2+} could decrease the tyrosine phosphorylation of CaM in RSV-transformed cells (*56*). In the current report, we used the cell-permeable Ca^{2+} sequestrant, BAPTA-AM, to study the role of Ca^{2+} in the activation of NHE-1 by 5-HT and Ang II in VSMC and, particularly, in the tyrosine phosphorylation of CaM by Jak2. Our data show that in VSMC, as in mIMCD-3 cells, the Ca^{2+} ionophore A23187 induces Jak2 phosphorylation (Figure 7A). This is in agreement with a recently published study by Frank et al., in which a requirement for Ca^{2+} in Ang II-induced activation of Jak2 in VSMC was demonstrated (*57*). It is noteworthy that the current work and our previous work (*18*) document that three distinct $G_{q/11}$-coupled receptors (bradykinin B_2, angiotensin AT_1, and serotonin $5\text{-}HT_{2A}$) use this pathway to activate NHE-1 in two different cell types. Thus, this pathway may be a fundamental mechanism through which $G_{q/11}$-coupled receptors rapidly activate NHE-1.

We further found that Ca^{2+} plays an essential role in the formation of a complex between Jak2 and CaM and in the tyrosine phosphorylation of CaM (Figure 7B,C). Interestingly, in our experiments there was a notable difference in the apparent magnitude of the involvement of Ca^{2+} in the effects of 5-HT and in those of Ang II. Pretreatment with BAPTA-AM essentially abolished 5-HT-induced ECAR (Figure 6), 5-HT-stimulated phosphorylation of Jak2, as well as complex formation between Jak2 and CaM, and subsequent phosphorylation of CaM (Figure 7). However, the same treatment only partially inhibited the same events initiated by Ang II (Figures 6 and 7). One possible explanation for this difference is that Ang II, in addition to a Ca^{2+}-dependent mechanism, may also use some Ca^{2+}-independent pathway for Jak2 activation. Such a possibility has been detailed by Doan et al., who demonstrated the ability of a modified AT_1 receptor, uncoupled from $G\alpha_{q/11}$ activation, to activate the Jak-STAT pathway in the absence of a G protein-coupled

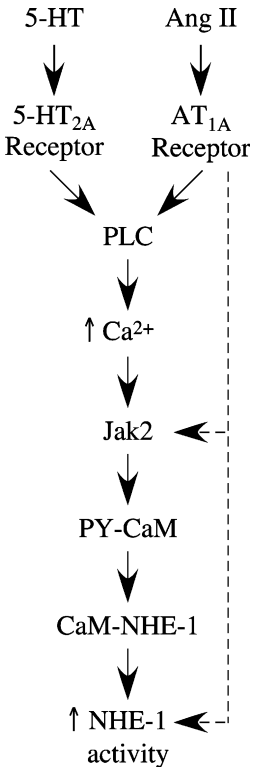

FIGURE 8: Proposed pathway of 5-HT- and Ang II-induced activation of NHE-1 in VSMC. This scheme is described in the Discussion section. The dashed line indicates a putative additional pathway used by Ang II to activate NHE-1.

rise in intracellular Ca^{2+} in transfected CHO cells (*58*). Another possible explanation is that the AT_{1A} receptor uses another pathway that bypasses CaM and Jak2 such as phosphorylation of serine 703 of NHE-1 by $p90^{rsk}$, as described by Takahashi and colleagues (*15*). These possibilities are outlined in the scheme shown in Figure 8.

In summary, we used primary cultures of rat aortic VSMC to examine the regulation of NHE-1 by two prototypical G protein-coupled receptors: the serotonin $5\text{-}HT_{2A}$ receptor and the angiotensin II AT_1 receptor. The current work shows that $5\text{-}HT_{2A}$ and AT_1 receptors, endogenous to VSMC, activate NHE-1 through a pathway that involves PLC, elevated intracellular Ca^{2+}, CaM, and Jak2. 5-HT and Ang II rapidly, and in a Ca^{2+}-dependent manner, (1) stimulate the assembly of a signal transduction complex that includes CaM, Jak2, and NHE-1 and (2) induce the tyrosine phosphorylation of CaM by Jak2. We propose that this pathway is a fundamental mechanism for the rapid regulation of NHE-1 by $G_{q/11}$ protein-coupled receptors in multiple cell types.

ACKNOWLEDGMENT

We thank Jana Fine for excellent technical assistance.

REFERENCES

1. Orlowski, J., and Grinshtein, S. (1997) *J. Biol. Chem. 272*, 22373−22376.
2. Wakabayashi, S., Shigekawa, M., and Pouyssegur, J. (1997) *Physiol. Rev. 77*, 51−74.
3. LaPointe, M. S., and Battle, D. C. (1994) *Am. J. Med. Sci. 307*, S9−S16.
4. Lucchesi, P., and Berk, B. C. (1995) *Cardiovasc. Res. 29*, 172−177.
5. Bobick, A., Grooms, A., Grinpukel, S., and Little, P. J. (1988) *J. Hypertens., Suppl. 6*, S219−S221.
6. Bertrand, B., Wakabayashi, S., Ikeda, T., Pouyssegur, J., and Shigekawa, M. (1994) *J. Biol. Chem. 269*, 13703−13709.
7. Fliegel, L., Walsh, M., Singh, D., Wong, C., and Barr, A. (1992) *Biochem. J. 282*, 139−145.
8. Snabaitis, A. K., Yokoyama, H., and Avkiran, M. (2000) *Circ. Res. 86*, 214−220.
9. Sauvage, M., Maziere, P., Fathallah, H., and Giraud, F. (2000) *Eur. J. Biochem. 267*, 955−962.
10. Tominaga, T., Ishizaki, T., Narumiya, S, and Barber, D. L. (1998) *EMBO J. 17*, 4712−4722.
11. Kusuhara, M., Takahashi, E., Peterson, T. E., Abe, J., Ishida, M., Han, J., Ulevitch, R., and Berk, B. C. (1998) *Circ. Res. 83*, 824−831.
12. Aharonovitz, O., and Granot, Y. (1996) *J. Biol. Chem. 271*, 16494−16499.
13. Bianchini, L., L'Allemain, G., and Pouyssegur, J. (1997) *J. Biol. Chem. 272*, 271−279.
14. Takahashi, E., Abe, J., and Berk, B. C. (1997) *Circ. Res. 81*, 268−273.
15. Takahashi, E., Abe, J., Gallis, B., Aebersold, R., Spring, D., Krebs, E. G., and Berk, B. C. (1999) *J. Biol. Chem. 274*, 20206−20214.
16. Sardet, C., Fafournoux, P., and Pouyssegur, J. (1991) *J. Biol. Chem. 266*, 19166−19171.
17. Wakabayashi, S., Bertrand, B., Shigekawa, M., Fafournoux, P., and Pouyssegur, J. (1994) *J. Biol. Chem. 269*, 5583−5588.
18. Mukhin, Y. V., Vlasova, T., Jaffa, A. A., Collinsworth, G., Bell, J., Tholanikunnel, B., Pettus, T., Fitzgibbon, W., Ploth, D. W., Raymond, J. R., and Garnovskaya, M. N. (2001) *J. Biol. Chem. 276*, 17339−17346.
19. Ng, L. L., Sweeney, F. P., Siczkowski, M., Davies, J. E., Quinn, P. A., Krolewski, B., and Krolewski, A. S. (1995) *Hypertension 25*, 971−977.
20. Rosskopf, D., Dusing, R., and Siffert, W. (1993) *Hypertension 21*, 607−617.
21. Lucchesi, P. A., DeRoux, N., and Berk, B. C. (1994) *Hypertension 24*, 734−738.
22. LaPointe, M. S., Ye, M., Moe, O. W., Alpern, R. J., and Battle, D. C. (1995) *Kidney Int. 47*, 78−87.
23. Ullian, M. E., and Fine, J. J. (1994) *J. Cell. Physiol. 161*, 201−208.
24. Touyz, R. M., and Schiffrin, E. L. (2000) *Pharmacol. Rev. 52*, 639−672.
25. Marrero, M. B., Schieffer, B., Bernstein, K. E., and Ling, B. N. (1996) *Clin. Exp. Pharmacol. Physiol. 23*, 83−88.
26. Xi, X. P., Graf, K., Goetze, S., Fleck, E., Hsueh, W. A., and Law, R. E. (1999) *Arterioscler., Thromb., Vasc. Biol. 19*, 73−82.
27. Touyz, R. M., He, G., Wu, X. H., Park, J. B., Mabrouk, M. E., and Schiffrin, E. L. (2001) *Hypertension 38*, 56−64.
28. Rocic, P., and Lucchesi, P. A. (2001) *J. Biol. Chem. 276*, 21902−21906.
29. Freeman, E. J. (2000) *Arch. Biochem. Biophys. 374*, 363−370.
30. Amiri, F., Venema, V. J., Wang, X., Ju, H., Venema, R. C., and Marrero, M. B. (1999) *J. Biol. Chem. 274*, 32382−32386.
31. Berk, B. C., Aronow, M. S., Brock, T. A., Cragoe, E., Jr., Gimbrone, M. A., Jr., and Alexander, R. W. (1987) *J. Biol. Chem. 262*, 5057−5064.
32. Ye, M., Flores, G., and Batlle, D. (1996) *Hypertension 27*, 72−78.
33. Rao, G. N., Sardet, C., Pouyssegur, J., and Berk, B. C. (1990) *J. Biol. Chem. 265*, 19393−19396.
34. Touyz, R. M., and Schiffrin, E. L. (1997) *Hypertension 30*, 222−229.
35. Fanburg, B. L., and Lee, S. L. (1997) *Am. J. Physiol. 272*, L795−L806.
36. Saxena, P. R. (1989) *Fundam. Clin. Pharmacol. 3*, 245−265.
37. van Zwieten, P. A., Blauw, G. J., and van Brummelen, P. (1990) *Br. J. Clin. Pharmacol. 30*, 69S−74S.
38. Corson, M. A., Alexander, R. W., and Berk, B. C. (1992) *Am. J. Physiol. 262*, C309−C315.
39. Watts, S. W., Yang, P., Banes, A. K., and Baez, M. (2001) *J. Cardiovasc. Pharmacol. 38*, 539−551.
40. Semenchuk, L. A., and Di Salvo, J. (1995) *FEBS Lett. 370*, 127−130.
41. Banes, A., Florian, J., and Watts, S. W. (1999) *J. Pharmacol. Exp. Ther. 291*, 1179−1187.
42. Watanabe, T., Pakala, R., Katagiri, T., and Benedict, C. R. (2001) *J. Vasc. Res. 38*, 341−349.

43. Garnovskaya, M. N., Gettys, T. W., van Biesen, T., Prpic, V., Chuprun, J. K., and Raymond, J. R. (1997) *J. Biol. Chem. 272*, 7770−7776.
44. Garnovskaya, M. N., Mukhin, Y., and Raymond, J. R. (1998) *Biochem. J. 330*, 489−495.
45. Garnovskaya, M. N., Nebigil, C. G., Arthur, J. M., Spurney, R. F., and Raymond, J. R. (1995) *Mol. Pharmacol. 48*, 230−237.
46. Saxena, R., Saksa, B. A., Fields, A. P., and Ganz, M. B. (1993) *Am. J. Physiol. 265*, F53−F60.
47. Prpic, V., Fitz, J. G., Wang, Y., Raymond, J. R., Garnovskaya, M. N., and Liddle, R. A. (1998) *Am. J. Physiol. 275*, G689−G695.
48. McConnell, H. M., Owicki, J. C., Parce, J. W., Miller, D. L., Baxter, G. T., Wada, H. G., and Pitchford, S. (1992) *Science 257*, 1906−1912.
49. Schroeder, K. S., and Neagle, B. D. (1996) *J. Biomol. Screening 1*, 75−80.
50. Boron, W. F. (1977) *Am. J. Physiol. 233*, C61−C73.
51. Seewald, S., Sachinidis, A., Dusing, R., Ko, Y., Seul, C., Epping, P., and Vetter, H. (1997) *Atherosclerosis 130*, 121−131.
52. Seewald, S., Schmitz, U., Seul, C., Ko, Y., Sachinidis, A., and Vetter, H. (1999) *Am. J. Hypertens. 12*, 532−537.
53. Di Salvo, J., and Raatz Nelson, S. (1998) *FEBS Lett. 422*, 85−88.
54. Rosen, B., Barg, J., and Zimlichman, R. (1999) *Am. J. Hypertens. 12*, 1243−1251.
55. Marrero, M. B., Schieffer, B., Li, B., Sun, J., Harp, J. B., and Ling, B. N. (1997) *J. Biol. Chem. 272*, 24684−24690.
56. Fukami, Y., Nakamura, T., Nakayama, A., and Kanehisa, T. (1986) *Proc. Natl. Acad. Sci. U.S.A. 83*, 4190−4193.
57. Frank, G. D., Saito, S., Motley, E. D., Sasaki, T., Ohba, M., Kuroki, T., Inagami, T., and Eguchi, S. (2002) *Mol. Endocrinol. 16*, 367−377.
58. Doan, T. N., Ali, M. S., and Bernstein, K. E. (2001) *J. Biol. Chem. 276*, 20954−20958.

BI034563+